FMRI BRAIN ACTIVITY AND UNDERLYING HEMODYNAMICS ESTIMATION IN A NEW BAYESIAN FRAMEWORK

David M. Afonso[1]
dafonso@isr.ist.utl.pt

João M. Sanches[1]
jmrs@isr.ist.utl.pt

Martin H. Lauterbach[2] *(MD)*
mlauterbach@fm.ul.pt

[1]Institute for Systems and Robotics - Instituto Superior Técnico, Lisbon, Portugal.
[1]Faculty of Medicine, University of Lisbon, Portugal.

ABSTRACT

The emerging functional MRI (*Magnetic Resonance Imaging*), *fMRI*, imaging modality was developed to obtain non-invasive information regarding the neural processes behind pre-determined task. The data is gathered in such a way that the extraction certainty of the desired information is maximized. Still this is a difficult task due to low Signal-to-Noise Ratio (SNR), corrupting noise and artifacts from several sources. The most prevalent method, here called *SPM-GLM* [1] uses a conventional statistical inference methodology based on the t-statistics, where it assumes a rather rigid shape on the BOLD *Hemodynamic Response Function* (HRF), constant for the whole region of interest (ROI).

A new algorithm, designed in a Bayesian framework, is presented in this paper, called *SPM-MAP*. The algorithm jointly detects the brain activated regions and the underlying HRF in an adaptative and local basis. This approach presents two main advantages: *1)* the activity detection benefits from the method's high flexibility toward the HRF shape; *2)* it provides local estimations for the HRF.

The *SPM-MAP* algorithm is validated by using Monte Carlo tests with synthetic data and comparisons with the *SPM-GLM* are also performed. Tests using real data are also performed and results are compared with the ones provided by the *SPM-GLM* method tuned by the medical doctor.

Index Terms— functional Magnetic Resonance, Nervous system, MAP estimation, Biomedical signal detection, Adaptive signal processing.

1. INTRODUCTION

Functional Magnetic Resonance Imaging (fMRI) is a new and powerful method that, among other purposes, may be used in the determination of which parts of the brain are involved in a particular task. It is sensitized to the paramagnetic properties of deoxyhaemoglobin [2] which concentration locally fluctuates in strong correlation with the physiological events of brain activity.

The computational analysis of the data provided by this method is difficult and is an open problem. Usually, it aims at obtaining a visual statistical map representation of the activated areas after the stimulation paradigm applied during the scan (see Fig. 1).

To obtain the desirable results several processing steps are usually involved, e.g. image preprocessing (motion compensation and noise removal), spacial normalization transformation, statistical tests and the final inferences procedures [3]. Considering the last two steps, which are the focus of this paper, most of the methods described in the literature are variants of the general linear model (GLM [1]), which express the observed BOLD response variable in terms of a linear combination of explanatory variables (EVs), and make use of classical statistics (T or F tests based on the null hypothesis) to infer activity, using e.g. a p-value threshold.

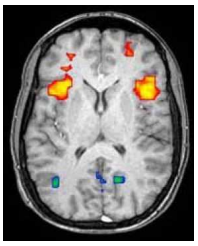

Fig. 1. Example of fMRI activated and non activated regions overlaid on a structural MRI image.

The main EVs used in the GLM allocate temporal variance in the (preprocessed) data with strong correlation with the paradigm stimulus. To achieve this, the stimulus paradigm timing is convolved with one or more fixed shape *hemodynamic impulse response function* (HRF). But since there is considerable variability in the HRF shape [4,5], this may lead to reduced sensitivity when the local HRF is significantly different from the template one. Also, the *SPM-GLM* method is based on the p-value tunned by the medical doctor which introduces a subjective factor on the final results.

To overcome these limitations this paper presents a new algorithm designed in a Bayesian framework based on the *Maximum A Posteriori* (MAP) [6] criterion. This new method combines the activity detection problem and the local HRF estimation problem, in order to minimize the detection error probability providing the best SPM result with the available data. The method is parameter free providing the most likely solution for the activation event at each location: activated or non activated, eliminating the subjectivity associated to the p-value selection in the *SPM-GLM* method. Additionally, it provides local estimations of the HRF which may be useful to understand the neuro-vascular and physiological events behind local brain activity.

Monte Carlo tests with synthetic data are performed, for comparison purposes with the *SPM-GLM* method and also for absolute assessment in order to statistically characterize the overall error probability. Detection analysis results on real fMRI block-designed data are also presented and comparison with the *SPM-GLM* results provided by the medical doctor is presented.

This work was supported by Fundação para a Ciência e a Tecnologia (ISR/IST plurianual funding) through the POS Conhecimento Program which includes FEDER funds.

2. PROBLEM FORMULATION

The *SPM-MAP* algorithm assumes the following data observation model at each time course,

$$y(n) = h(n) * \underbrace{\sum_{k=1}^{N} \beta_k p_k(n)}_{x(n)} + \eta(n) \quad (1)$$

where $\eta(n)$ is modeled as *Additive White Gaussian Noise* (AWGN), $h(n)$ is the HRF of the brain tissues, $p_k(n)$ are the paradigm stimulus signals along time and β_k are unknown binary variables to model the activation of the voxel by the k[th] stimulus.

The estimation process is performed by minimizing the following energy function depending on the binary unknowns β_k, on the hemodynamic response $h(n)$, and on the observations $y(n)$,

$$E(\mathbf{y}, \mathbf{x}(\mathbf{b}), \mathbf{h}) = E_y(\mathbf{y}, \mathbf{x}(\mathbf{b}), \mathbf{h}) + E_b(\mathbf{b}) + E_h(\mathbf{h}) \quad (2)$$

where the *data fidelity term* is

$$E_y(\mathbf{y}, \mathbf{x}(\mathbf{b}), \mathbf{h}) = -\log(p(\mathbf{y}|\mathbf{x}(\mathbf{b}), \mathbf{h})) \quad (3)$$

and the prior terms associated to the unknowns to be estimated, $\mathbf{b} = \{\beta_1, ...\beta_N\}$ and $\mathbf{h} = \{h(0), ..., h(j-1)\}$ are

$$E_b(\mathbf{b}) = -\log(p(\mathbf{b})) \quad (4)$$

$$E_h(\mathbf{h}) = -\log(p(\mathbf{h})). \quad (5)$$

where j is selected to cover 40 seconds of HRF.

These priors incorporate the *a priori* knowledge about the unknowns to be estimated: *i)* β_k are binary and *ii)* $h(n)$ is smooth.

Assuming statistical independence of the observations

$$p(\mathbf{y}|\mathbf{x}(\mathbf{b}), \mathbf{h}) = \prod_{i=1}^{L} p(y(i)|(x * h)(i)) \quad (6)$$

where $p(y(i)|(x*h)(i)) = \frac{1}{\sqrt{2\pi {\sigma_\eta}^2}} e^{-\frac{(y(i)-(x*h)(i))^2}{2{\sigma_\eta}^2}}$ and ${\sigma_\eta}^2$ is the energy of the noise. The parameters β_k to be estimated are also assumed independent,

$$p(\mathbf{b}) = \prod_{i=1}^{N} p(\beta_k) \quad (7)$$

where $p(\beta_k)$ is a bi-modal distribution defined as a sum of two Gaussian distributions centered at zero and one, with variance ${\sigma_\beta}^2$

$$p(\beta_k) = \frac{1}{2}\left[N(0, \sigma_\beta^2) + N(1, \sigma_\beta^2)\right] \quad (8)$$

because β_k are binary variables, $\beta_k \in \{0, 1\}$. In order to better approximate the binary answer, the σ_β parameter should be as small as possible but numerical stability reasons prevent the adoption of too small values. The prior term $E_b(b)$ may therefore be written as

$$E_b(\mathbf{b}) = \sum_{k=1}^{N} \left[\frac{2\beta_k^2 - 2\beta_k + 1}{4\sigma_\beta^2} - \log\left(\cosh\left[\frac{2\beta_k - 1}{4\sigma_\beta^2}\right]\right)\right].$$

To impose smoothness [7] on the estimated hemodynamic response, $h(n)$ is assumed to be a *Markov Random Field* (MRF), which means, by the Hammersley-Clifford theorem, that $p(\mathbf{h})$ is a *Gibbs* distribution. In this paper a Gibbs distribution with quadratic potential functions is used

$$p(\mathbf{h}) = \frac{1}{Z_h} e^{-\alpha \sum_{n=2}^{N} (h(n) - h(n-1))^2}. \quad (9)$$

Besides the smoothness of $h(n)$ it is also assumed that $h(n)$ is the impulse response of the following *Infinite Impulse Response* (IIR) *Physiologically Based Hemodynamic* (PBH) model [8],

$$H(z) = \frac{b_0 + b_1 z^{-1} + b_2 z^{-2}}{1 + a_1 z^{-1} + a_2 z^{-2} + a_3 z^{-3}} \quad (10)$$

where the coefficients b_k and a_k must be estimated.

Therefore, after a first step where a temporal smoothed finite response (FIR) version of $\mathbf{h}$, $\mathbf{g}$, is estimated, an infinite impulse response (IIR) is computed by projecting $\mathbf{g}$ in the space of admissible responses of (10).

The overall estimation process is therefore iteratively performed in the following three steps,

$$\mathbf{b}^t = \arg\min_{\mathbf{b}} E(\mathbf{y}, \mathbf{x}(\mathbf{b}^{t-1}), \mathbf{h}^{t-1}) \quad (11)$$

$$\mathbf{g} = \arg\min_{\mathbf{h}} E(\mathbf{y}, \mathbf{x}(\mathbf{b}^{t}), \mathbf{h}^{t-1}) \quad (12)$$

$$\mathbf{h}^t = \text{Proj}_{FIR}\left[\text{Proj}_{IIR}(\mathbf{g})\right] \quad (13)$$

where $()^t$ means estimation at t^{th} iteration and $Proj$ stands for the projection operation by using the *minimum square error* (MSE) criterion. The Proj_{IIR} problem is not trivial [9,10]. In this paper the approximation algorithm proposed by *Shanks* [11,12] is used.

The above three steps are iteratively performed until convergence is achieved.

3. RESULTS

This section presents the test results done on the *SPM-MAP* method and is divided is three sections, where synthetic data is used in the first two and experimental data in the last.

3.1. *SPM-MAP* v.s. *SPM-GLM* Activity Detection

To access the effectiveness of the proposed *SPM-MAP* method against the presented *SPM-GLM*, synthetic 1D-block-designed single stimulus data, corrupted by several amount of AWGN energies, σ_η, and several stimulus epochs (periods in a block design paradigm approach), N, are used in Monte Carlo simulations. In these, the *error probability* (P_e), was obtained for each method as the ratio of the total number of wrong estimations over the total number of Monte Carlo tests (250). In this first experiment the HRF is assumed to be known and was selected from the PBH model estimation on real data [8].

The resulting P_e differences between *SPM-MAP* and *SPM-GLM*, i.e.: $\Delta P_e = P_{e(SPM-MAP)} - P_{e(SPM-GLM)}$, was computed for each experiment, and the average results for the different noise levels and epochs are displayed in Fig.2 Although the performance of both algorithms decreases, as expected, with the amount of noise and with the decrease in epochs number, the ΔP_e obtained is negative for most of the pair parameters (N, σ) tested, $\sum_{i,j} \Delta P_e(N_i, \sigma_j) = -0.46$ (the volume under the graph displayed in Fig.2). The number of negative values of ΔP_e, $\#(\Delta P_e < 0) = 23$ and the number of positive values of ΔP_e, $\#(\Delta P_e > 0) = 6$ which means that the *SPM-MAP* outperforms the *SPM-GLM* method for almost every configuration tested.

It is important to notice that in the *SPM-GLM* approach, the HRF is indirectly estimated and used for every time-course activation analysis. On the contrary, in the *SPM-MAP* method, this HRF

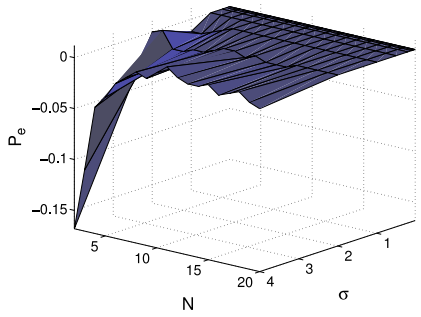

Fig. 2. Error probability differences, ΔP_e, between the *SPM-MAP* and the *SPM-GLM* methods. N is the number of paradigm epochs and σ is the AWGN standard deviation level.

is jointly estimated with the activation variables in an adaptative and space variant basis. The adaptatively nature of the *SPM-MAP* method clearly suggests that in real conditions the performance gap between both methods increases.

3.2. Joint Activity Detection and HRF Estimation Results

In this sub section synthetic data is used to characterize the *error probability*, P_e, of the *SPM-MAP* method. Two synthetic binary images of 128x128 voxels where generated, which represent a single BOLD slice signal and the activation ground truth of two paradigm stimulus to be estimated for each voxel. For each voxel, synthetic block-designed data was generated with 5 paradigm epochs, several noise levels and a fixed HRF extracted from real data. The mean P_e is presented in Tab. 1 for each noise level.

σ_η $SNR(dB)$	0.2 [7.3,11]	0.5 [-0.63,2.6]	0.7 [-3.6,-0.37]	1 [-6.7,-3.5]
$P_e(\%)$	0.0427	0.0916	0.168	4.27
$\dot{P}_e(\%)$	0	0	0.0244	1.51
$\ddot{P}_e(\%)$	0	0	0.0073	0.513

Table 1. Monte Carlo P_e of *SPM-MAP* for several noise levels (displayed in the σ_η and SNR lines for two different signal energy situations, $\sum_{k=1}^{2} \beta_k = 1$ and $\sum_{k=1}^{2} \beta_k = 2$. Spatial correlation correction is exemplified in $\dot{P}_e$ and $\ddot{P}_e$ where one and two isolated pixels were dismissed, respectively.

It is important to point-out that although the SNR in MRI depends on a large number of variables, it is usually more than $1dB$ [3]. So the most realistic σ_η values would be situated between 0.2 and 0.5, for the data used (see Table 1). In this range the method achieves values of $P_e < 0.1\%$. Furthermore, for the very high noise amount of $\sigma_\eta = 1$ ($SNR = [-6.7; -3.5]$) the P_e stays below 5%.

For illustration purposes, the P_e is recalculated after a simple clustering correction of removing areas of one ($\dot{P}_e$) and two ($\ddot{P}_e$) isolated voxels in an 8 voxels neighborhood. The resultant error probabilities (see Table 1) decreases for all the noise amounts, yielding null for $\sigma_\eta = 0.2$ and $\sigma_\eta = 0.5$.

The P_e results cannot be directly compared with the results in section 3.1 because *i)* there are two paradigms instead of one and *ii)* the HRF is unknown and jointly estimated; yielding an explosion in the possible number of solutions.

3.3. Joint Activity Detection Results On Real Data

In this section results using real data are presented an compared with the ones obtained by the medical doctor by using the *Brain Voyager* software.

Subjects and Data Collection

Two volunteers with no history of neurological or psychiatric diseases participated on motor and trajectory generation block-designed paradigms during fMRI data acquisition on a *Philips Intera Achieva Quasar Dual 3T* whole-body system with a 8 channel head-coil. T2*-weighted echo-planar images (EPI), 23cm square field of view with a 128×128 matrix size resulting in an in-plane resolution of $1.8 \times 1.8mm$ for each $4mm$ slice, echo time = $33ms$, flip angle = 20^o were acquired with a $TR = 3000ms$.

Data Analysis and Results The fMRI data was preprocessed with the standard procedures implemented in the *Brain Voyager* software, namely decrease of data distortions due to motion or other phase changes over time (registration) and spacial smoothing. This data was then statistically processed by the *Brain Voyager SPM-GLM* and *SPM-MAP* algorithms, and the results are plotted in Fig. 3 for a selection of two slices presenting considerable activity areas. Since the obtainable brain maps by *SPM-GLM* highly depends on the selected p-values (see section 3.1), a neurologist provided the results (up right), for each data set, which he considers more correct (*reference* result), based on its experience. Since this result is subjective, he also provided two other results which he considers *loose* (bottom left) and *restricted* (bottom right).

Visual inspection of the results in Fig. 3 show some expected resemblance between the preferred solution of the neurologist, obtained with the *SPM-GLM* algorithm, and the brain maps obtained by the proposed *SPM-MAP* algorithm. The small differences displayed in Figs. 3 (a) and (b) and may be explained by the structural different approaches used by both methods about the HRF. In the *SPM-GLM* this response is considered space invariant while in the *SPM-MAP* methods it is jointly estimated in each time course.

In several of the brain map image sets there are brain regions detected as activated by *SPM-MAP* that were not detected by *SPM-GLM* as shown in Fig.4. These are unlikely false positives. Considering that the error probability has been shown considerably low (see section 3.2), the probability of several false positives occurring grouped in a small image area, instead of randomly dispersed in the image, is infinitesimally small. Therefore, non single voxel brain areas detected by the proposed method should be considered as reliable as larger is its dimensions. The detection of these "new" areas happens when a voxel time-course does fluctuates in correlation with the stimulus paradigm, but with a different HRF from the template shape used by the *SPM-GLM*. Further anatomical testings are required to enhance confidence in these "new" areas. Furthermore, as shown in the Fig.4 the time course associated with these regions are clearly correlated with the paradigm as visually may be checked.

4. CONCLUSIONS

In this paper a new Bayesian method is proposed, where the neural activity detection is jointly obtained along with the HRF estimation. This approach presents two main advantages: *1)* the activity detection benefits from the adaptative nature of the HRF shape estimation and *2)* it provides local, space variant, HRF estimation. This might provide a useful tool to evaluate and compare estimated brain activity between regions or subjects and for possible behavioral, neural and vascular local consideration.

Furthermore, when comparing with the widespread *SPM-GLM* method, this new method does not depend on any tunning parameter, which means, the subjective nature of the results associated with the selection of a parameters by the medical doctor is removed in the proposed method.

Monte Carlo tests on synthetic-1D-block-designed data showed that the *SPM-MAP* algorithm outperforms the activity detection of

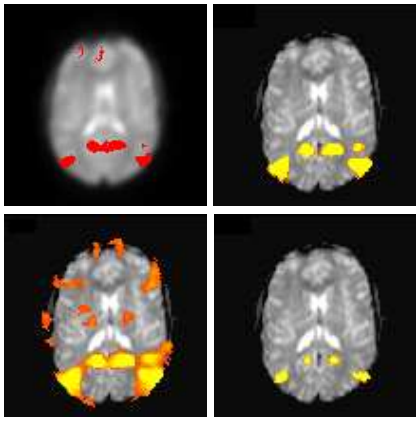

(a) Trajectory generation paradigm results.

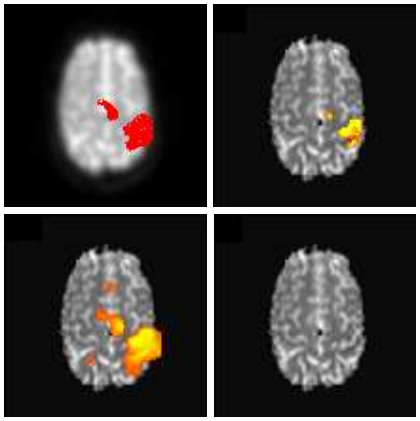

(b) Right hand paradigm results

Fig. 3. *SPM-MAP* activity detection SPM results (top left) on real data compared against data processed by a neurologist on *SPM-GLM* (top right - *reference* SPM result; bottom - *restricted* and *loose* SPM results).

the standard *SPM-GLM* method for almost every tested conditions: different noise levels, σ_j and number of paradigm epochs, N_i, in a block design framework.

The Monte Carlo tests performed to assess the performance of the algorithm have shown that the error probability obtained was lower than 0.1% for noise levels close to expected real ones, but even for extreme noise levels the method showed itself considerably reliable, presenting error probabilities lower than 5%.

The real fMRI data tests showed that the *SPM-MAP* was able to detect most of the activity detected by *SPM-GLM* and also detect other activated brain regions. Further analysis of these new brain areas will be done in future works.

5. REFERENCES

[1] K. J. Friston, "Analyzing brain images: Principles and overview," in *Human Brain Function*, R.S.J. Frackowiak and K.J. Friston and C. Frith and R. Dolan and J.C. Mazziotta, Ed., pp. 25–41. Academic Press USA, 1997.

[2] S. Ogawa, R. S. Menon, D. W. Tank, S. G. Kim, H. Merkle, J. M. Ellermann, and K. Ugurbil, "Functional brain mapping by blood oxygenation level-dependent contrast magnetic resonance imaging. A comparison of signal characteristics with a biophysical model," *Biophys J*, vol. 64, no. 3, pp. 803–812, Mar 1993, Comparative Study.

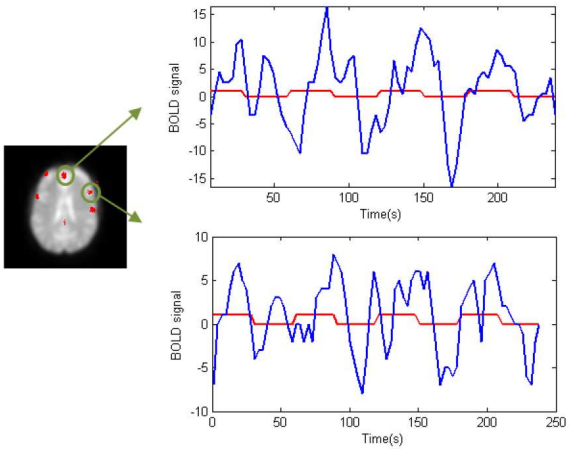

Fig. 4. Non detect areas with the *SPM-GLM* method.

[3] P. Jezzard, P. M. Matthews, and S. M. Smith, *Functional magnetic resonance imaging: An introduction to methods.*, Oxford Medical Publications, 2006.

[4] G. K. Aguirre, E. Zarahn, and M. D'esposito, "The variability of human, BOLD hemodynamic responses," *Neuroimage*, vol. 8, no. 4, pp. 360–369, Nov 1998, Clinical Trial.

[5] Daniel A. Handwerker, John M. Ollinger, and Mark D'Esposito, "Variation of BOLD hemodynamic responses across subjects and brain regions and their effects on statistical analyses," *Neuroimage*, vol. 21, no. 4, pp. 1639–1651, Apr 2004.

[6] K. M. Hanson, "Introduction to Bayesian image analysis," *Medical imaging VII: image processing (ed. M. H. Loew), Proc. SPIE*, vol. 1898, no. 8, pp. 716–731, 1993.

[7] Todd K. Moon and Wynn C. Stirling, *Mathematical methods and algorithms for signal processing*, 2000.

[8] David Miguel Afonso, João Sanches, and Martin Hagen Lauterbach, "Neural physiological modeling towards a hemodynamic response function for fMRI," *Conf Proc IEEE Eng Med Biol Soc*, vol. 1, pp. 1615–1618, 2007.

[9] Nikola Vucic and Holger Boche, "Equalization for MIMO ISI Systems using Channel Inversion under Causality, Stability and Robustness Constraints," in *Proc. IEEE International Conference on Acoustics, Speech, and Signal Processing (ICASSP 2006)*, Toulouse, France, May 2006.

[10] S. S. Rao and A. Ramasubrahmanyan, "Evolving iir approximants for fir digital filters," in *ASILOMAR '95: Proceedings of the 29th Asilomar Conference on Signals, Systems and Computers (2-Volume Set)*, Washington, DC, USA, 1995, p. 976, IEEE Computer Society.

[11] John L. Shanks, "Recursion filters for digital processing," *Geophysics*, vol. 32, pp. 33–51, 1967.

[12] Monson H. Hayes, *Statistical Digital Signal Processing and Modeling*, Wiley, March 1996.